Mekanika: Majalah Ilmiah Mekanika

Finite Element Modeling of Thickness Reduction and Displacement Behavior in 316L Stainless Steel Plates Under Corrosion States

Oleksiy Melnyk¹, Daffa Putra Islami², Ristiyanto Adiputra^{3*}

- 1 Department of Navigation and Maritime Safety, Odesa National Maritime University, Odesa, Ukraine
- 2 Department of Research and Development, PT. Dimonitor Indonesia Sejahtera, Surakarta, Indonesia
- 3 Research Center for Hydrodynamics Technology, National Research and Innovation Agency, Surabaya, Indonesia
- *Corresponding Author's email address: ristiyanto.adiputra@brin.go.id

Keywords:
Corrosion
Finite element method
Thickness reduction
Displacement behavior

Abstract

Structural steel corrosion is a critical engineering problem that can lead to catastrophic failures, resulting in loss of life, environmental harm, and substantial economic damage. Notable incidents, such as offshore platform collapses and ship hull breaches, have demonstrated the severe consequences of undetected or underestimated corrosion. In marine environments, crevice corrosion presents a particularly challenging case, as confined chemical conditions and the presence of barnacles promote localized degradation. Barnacles generate microcracks that accelerate the deterioration process. However, finite element modeling of crevice corrosion remains scarce and often relies on oversimplified geometries, which limits the accuracy in capturing actual corrosion volume, depth, and affected area. This study develops a 3D finite element model of barnacle-induced crevice corrosion on 316L stainless steel plates, based on long-term immersion data. Corrosion geometries were analyzed using laser scanning microscopy, with the analytical mapped field feature applied under transverse loading and random pit positions for exposure durations of 6, 12, and 36 months. The results reveal progressive increases in displacement (up to 17.27%), strain (30.8%), and stress (20.12%) compared to uncorroded plates, underscoring the substantial impact of localized corrosion on structural performance.

1 Introduction

Corrosion of structural steel poses a critical global challenge, with substantial financial and safety implications. In the United States alone, the annual cost of corrosion is estimated at USD 276 billion, equivalent to 3.1% of its Gross Domestic Product (GDP). In China, losses amount to approximately USD 310 billion, or 3.34% of the country's GDP [1,2]. These figures underscore the significant economic burden imposed on sectors such as transportation, infrastructure, and marine structures. A common manifestation of corrosion damage is the development of irregular surface pits, which act as stress concentrators and significantly reduce structural capacity. Several recent studies have reported serious incidents in marine and offshore structures resulting from corrosion-related failures, including hull damage, oil leakage, and localized structural collapse.

https://dx.doi.org/10.20961/mekanika.v24i2.102853

Revised 25 September 2025; received in revised version 25 September 2025; Accepted 25 September 2025 Available Online 17 October 2025

2579-3144

These incidents have resulted in operational downtime, substantial economic losses, and, in some cases, human casualties, underscoring the urgent need for a deeper understanding and more accurate modeling of the effects of corrosion on structural components. For example, fatigue strength degradation in corroded carbon steel can reach 50-90% compared to uncorroded specimens [3]. Moreover, finite element analyses of steel specimens exposed to atmospheric corrosion for four years have demonstrated Stress Concentration Factors (SCF) as high as 3.0 in localized pits [3], indicating a critical risk of fatigue crack initiation in corroded zones. These conditions underscore the urgent need for in-depth investigation into the mechanical consequences of corrosion on structural components, particularly under realistic long-term exposure scenarios. Crevice corrosion is classified as a form of localized corrosion [4].

This is a localized form of attack that shares numerous similarities with pitting corrosion, fatigue corrosion, and stress corrosion cracking. The corrosion results from disparate chemical conditions between the interior of a narrow crevice and the surrounding exposed metal surface [5]. This corrosion may manifest naturally or as a consequence of interconnections between components. This phenomenon is prevalent in marine environments due to the high oxygen, chloride ions, and moisture levels that accelerate electrochemical reactions within the corrosion pit [6]. A frequently overlooked yet substantial contributing factor pertains to the presence of marine organisms, such as barnacles, affixed to metal surfaces [7]. Barnacles have been observed to exhibit a remarkable capacity for adhesion, which can result in the formation of micro-cracks between their exoskeletons and the underlying metal substrates. These micro-cracks, in turn, have been shown to trigger differences in oxygen concentration, leading to the emergence of anaerobic areas [8]. These conditions have been shown to accelerate localized corrosion processes through corrosion mechanisms. This phenomenon, if left unaddressed, can potentially compromise the metal's structural integrity over time [9].

Several studies have been conducted to determine the corrosion resistance of metals. These studies have employed experimental testing of ship structural members in compressive tests [10] and bending tests [11]. Pitting is a process that can be defined as the deterioration of materials caused by the action of corrosion. The creation of artificial pits can accelerate this deterioration through drilling. The most recent developments in the field have involved the use of finite element method testing, specifically pitting corrosion modeling with analytically mapped field features, in ABAQUS software [12]. Although corrosion issues, especially crevice corrosion, have a significant impact, modeling crevice corrosion using the Finite Element Method (FEM) remains scarce. Existing studies often rely on simplified conventional pit geometries, which do not fully represent the actual volume, depth, and area identity of the corrosion [13]. To overcome this discrepancy, this study aims to conduct a thorough investigation into the effective implementation of corrosion modeling that accurately identifies volume, depth, and area [14]. Specifically, this study will model and evaluate 316L stainless steel plates that have experienced the effects of crevice corrosion due to barnacle attachment, based on long-term immersion test data. This modeling will be conducted through transverse loading simulations to obtain the mechanical response that occurs after the corrosion effect is applied [15]. The results of this study are expected to provide a valuable foundation for further examination of corrosion configurations in a specific model scale, as well as being of significant benefit to researchers aiming to develop more effective corrosion modeling methods.

Several previous studies have modeled the mechanical effects of corrosion using idealized shapes and manually arranged pit distributions. For instance, Sharifi et al. applied uniformly arranged semi-circular pits with a fixed diameter to evaluate stress responses in corroded plates [16]. Zhao et al. extended this by designing artificial pits with more varied geometries, such as cones, tubes, and semicircles, yet still relied on pre-defined artificial patterns [17]. In contrast, Pratama et al. introduced a mapped-field approach using real-world data by interpolating measured corrosion depths directly into the finite element mesh, thereby allowing for a more accurate simulation of corrosion morphology [18]. Building upon this, the present study integrates mapped corrosion profiles from long-term immersion tests in marine biofouling conditions, which remain largely unexplored in the literature.

This method enables the reproduction of complex and irregular crevice corrosion patterns into the finite element model, offering better realism in stress localization and mechanical degradation analysis. This study is therefore essential to advance the current understanding of structural behavior under crevice corrosion caused by marine biofouling, a condition that remains underrepresented in existing FEM-based research. Thus, this study makes a novel contribution by integrating experimentally derived corrosion profiles into finite element models through mapped-field geometry. This approach enables a more realistic simulation of crevice corrosion in stainless steel plates, allowing for a precise evaluation of stress localization and degradation due to biofouling-induced corrosion. To the authors' knowledge, the combination of mapped corrosion profiles with crevice attack scenarios under marine biofouling conditions remains underexplored in the existing literature, thus highlighting the novelty and practical contribution of this work.

2 Numerical Methods

2.1 Pit data

The geometry data of corrosion pits on the surface of stainless steel degraded by crevice corrosion is derived from three-dimensional corrosion morphology research conducted using laser scanning microscopy on the submerged plate surface. The material used in this modeling study is the same type of 316L stainless steel employed in the long-term immersion test for barnacle-induced corrosion [15]. As illustrated in Figure 1, the depth data for each well are presented over immersion periods of 6, 12, and 36 months.

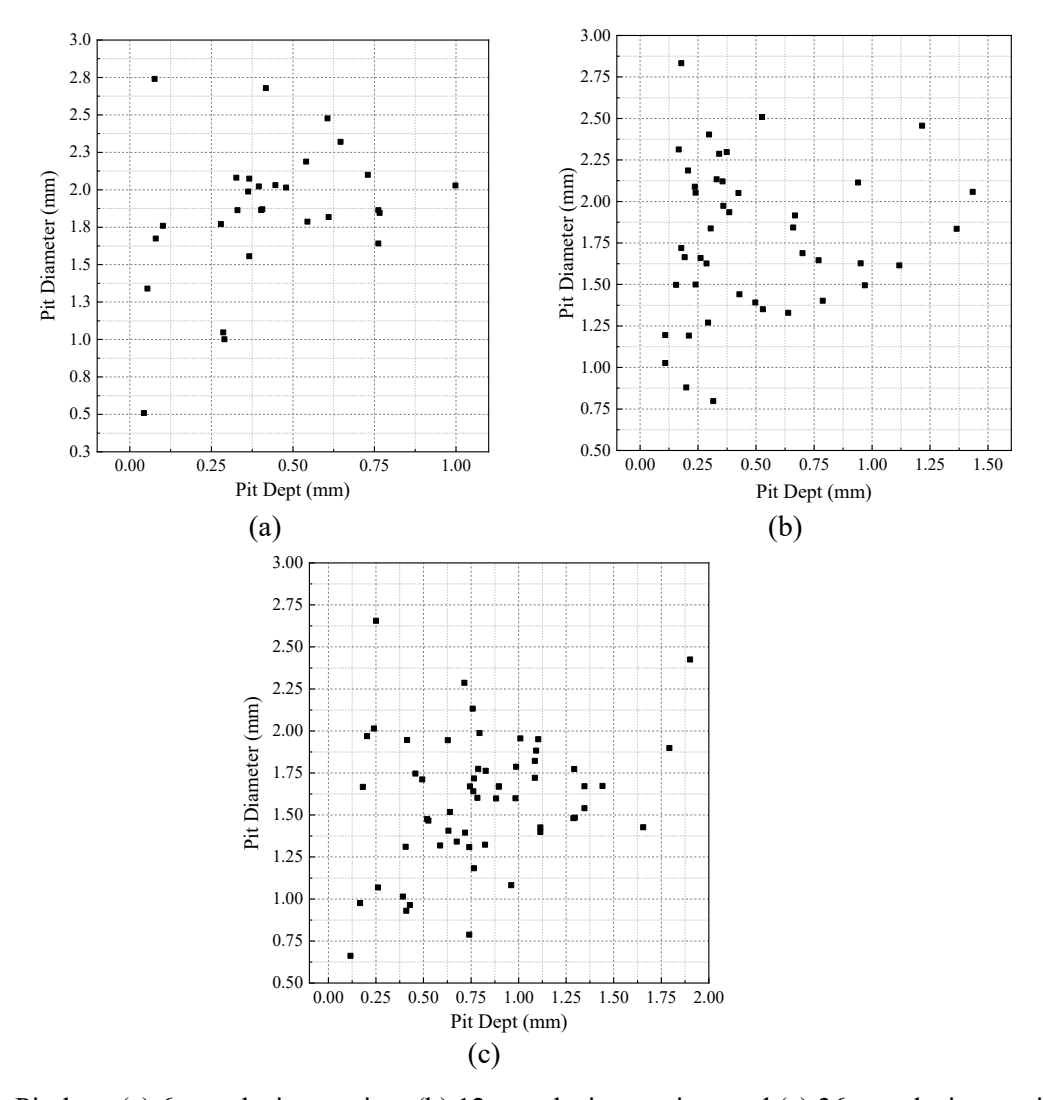


Figure 1. Pit data: (a) 6 months immersion, (b) 12 months immersion, and (c) 36 months immersion

2.2 Material type

The material applied in this modeling uses the same type of 316L stainless steel material as in the long-term immersion testing of barnacle-induced corrosion [15]. This objective is to ensure the reliability of the experimental data while also considering the impact of natural corrosion degradation on the type of material utilized. The material properties of 316L stainless steel are presented in Table 1.

	1 1	
Description	Value	Unit
density	8 × 10 ⁻⁴	kg/m ³
Young's modulus	193×10^{3}	MPa
Poisson's ratio	0.27	
ultimate tensile strength	485	MPa
yield strength	170	MPa
elongation at break	40	%

Table 1. Mechanical properties of 316L SS [18]

2.3 Corrosion modelling

The initial step in the corrosion modeling was the definition of the plate geometry and its discretization into finite elements. A square plate with dimensions of $50 \times 50 \times 3$ mm was generated to represent the specimen. For clarity, an engineering drawing of the plate, including its length, width, and thickness, is provided in Figure 2. The finite element mesh employed the S4R shell element, a four-node quadrilateral element with reduced integration and hourglass control, which is widely used for analyzing thin to moderately thick plates. This choice ensures a balance between computational efficiency and accuracy in capturing bending behavior. Specific elements within the mesh were designated as pit regions to represent crevice corrosion. At the same time, Figure 3 illustrates the nodal arrangement of the S4R element and the assignment of pit areas on the modeled plate surface.

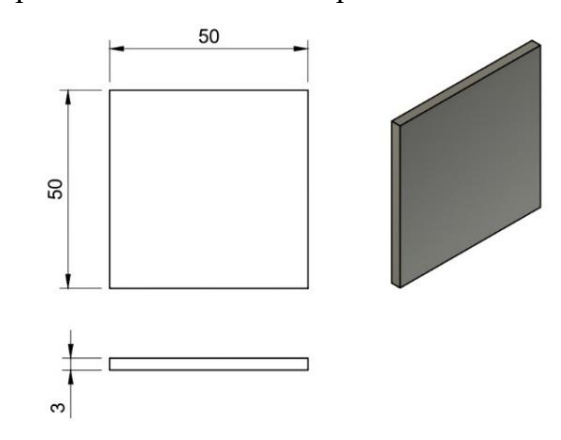


Figure 2. Plate specimen dimensions

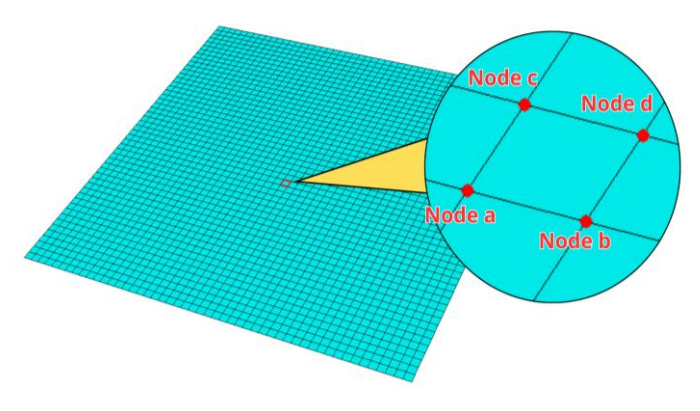


Figure 3. The following represents the position of the node on the element

To determine the mapping of each node on the model, it is essential to analyze the numerical pattern of the nodes by verifying it in ABAQUS. The element size has been set to 1 element equal to 1 mm². The nodes of the model are arranged in both vertical and horizontal directions according to the direction of the element's numbering. The utilization of a combination of both vertical and horizontal numeration patterns facilitates the systematic determination of node information coordinates. These coordinates are instrumental in determining the center and range area of each pit previously defined in each element. After describing the node information coordinates, the subsequent process involves converting the pit determination data in this model. This results in the conversion of the data into a point data format (x, y, z, field value) within the analytical mapped field feature. The results of the modeling are exhibited in the thickness section, as illustrated in Figure 4.

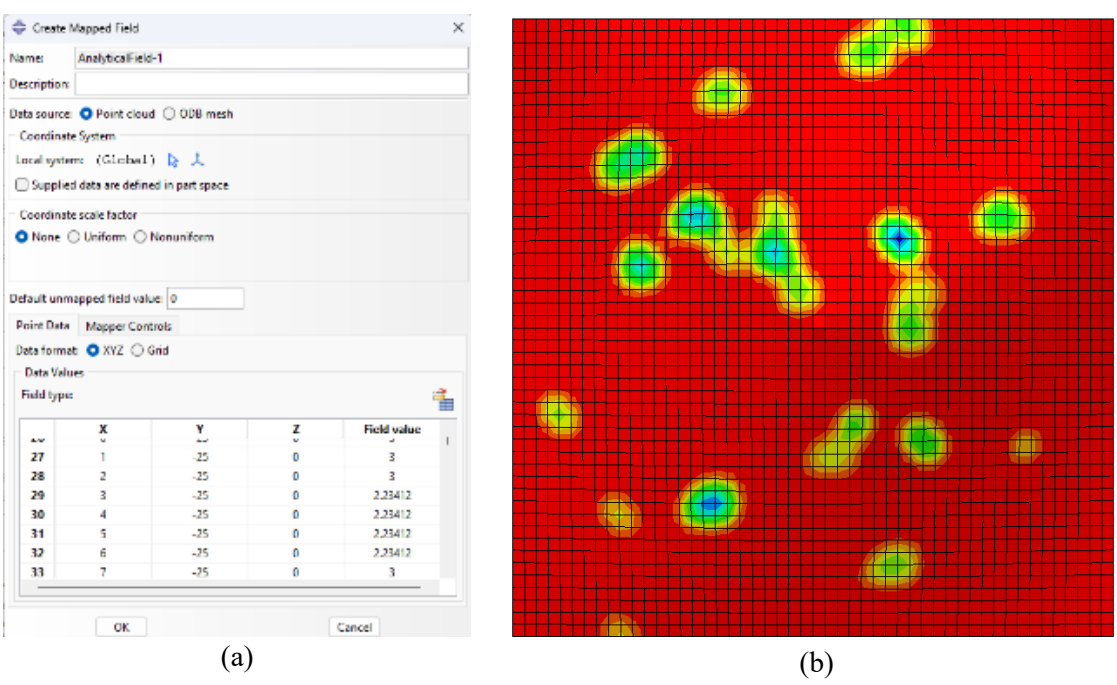


Figure 4. Corrosion modelling: (a) Point data and (b) Cross-sectional thickness on the corroded plate

2.4 Mechanical response method

A static analysis approach was undertaken to assess the behavior of the corroded plates when receiving perpendicular loads, illustrating the ship grounding scenario [19]. In this simulation, the load is represented by a concentrated load of 14.47 N. This value represents the load applied during the experiment and is determined by applying a scale-down factor based on fixed proportions. The boundary conditions used in this simulation are the same as those used for the impact phenomenon from the seabed on the plate attached to the idealized hull structure. The boundary condition applied is a simple support with restrictions in all displacement directions (U1 = U2 = U3 = 0) on all four sides of the plate.

2.5 Workflow of the study

To provide a concise overview of the research methodology, a workflow diagram is presented in Figure 5. This flowchart illustrates the sequential stages of the study, beginning with the literature review and specimen design in ABAQUS, followed by model benchmarking to ensure simulation accuracy. It then proceeds to corrosion data analysis, including the processing of crevice corrosion parameters such as pit depth, pit diameter, and number of pits. The subsequent stage involves generating random corrosion configurations, determining pit locations and sizes, and applying them to the finite element model using the analytical mapped field technique in ABAQUS. The process concludes with numerical simulations that incorporate variations of crevice corrosion effects, data processing, and the derivation of conclusions. Each step corresponds to the detailed descriptions provided in Sections 2.1 to 2.4.

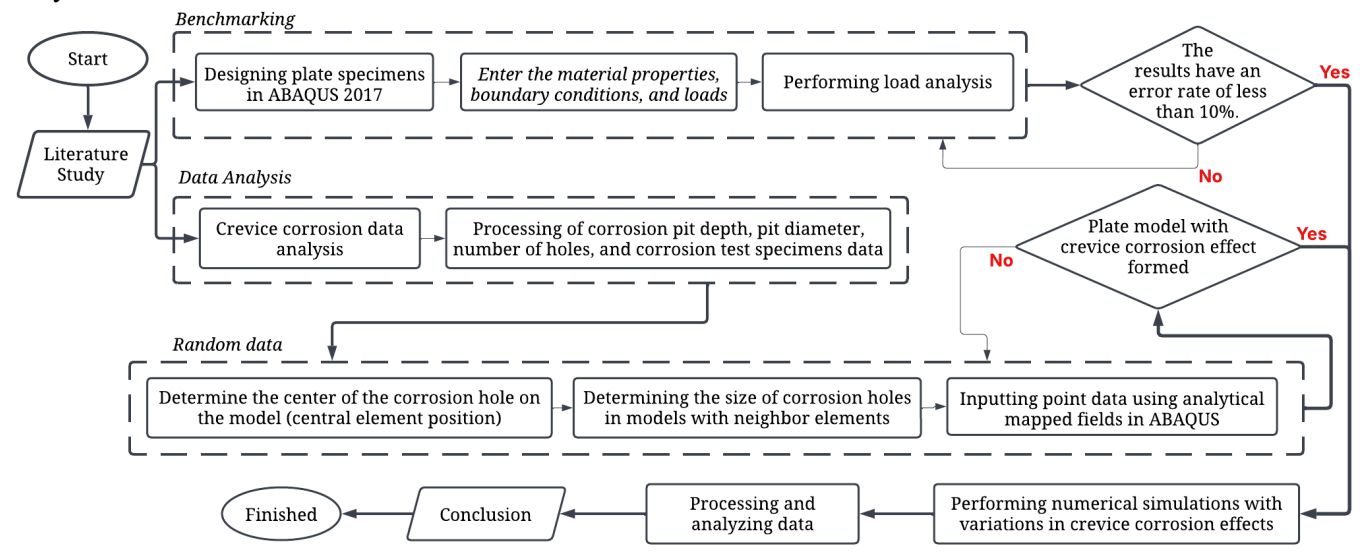


Figure 5. Numerical simulation flowchart

3 Result and Discussion

3.1 Thickness contour of corroded plate

The evaluation of plate thickness distribution due to corrosion was conducted to analyze the randomized pit modeling. The randomization process was carried out by establishing distinct pit center positions while maintaining constant pit volumes for each randomized set. As illustrated in Figures 6-8, the simulation contours demonstrate the variations in four sets of randomized pits (Set 1 to Set 15) for immersion periods of 6, 12, and 36 months, respectively.

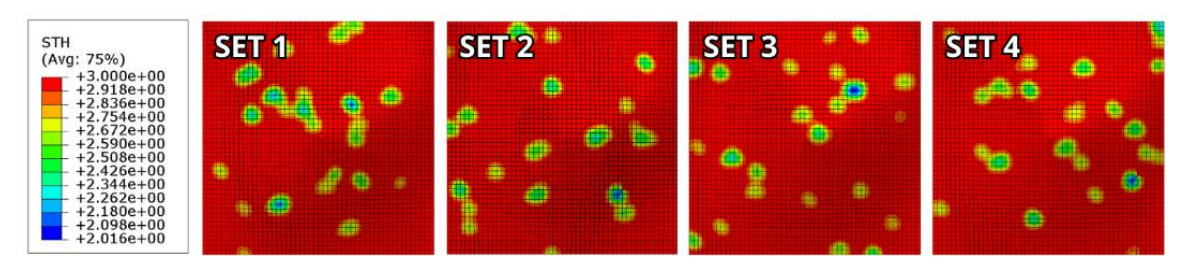


Figure 6. Thickness contour of a 6-month-immersed corroded plate

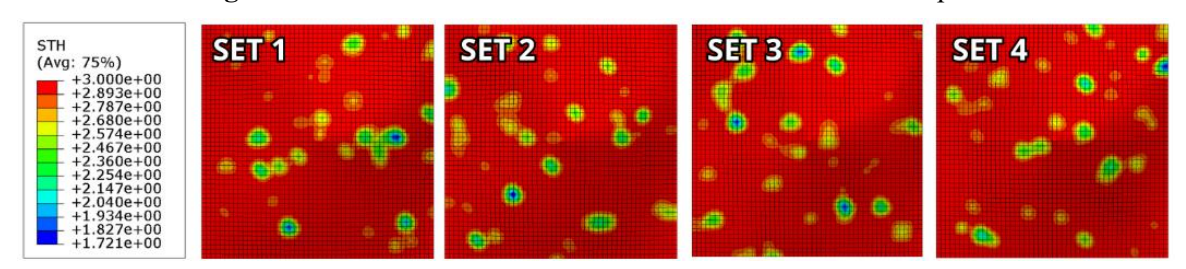


Figure 7. Thickness contour of a 12-month-immersed corroded plate

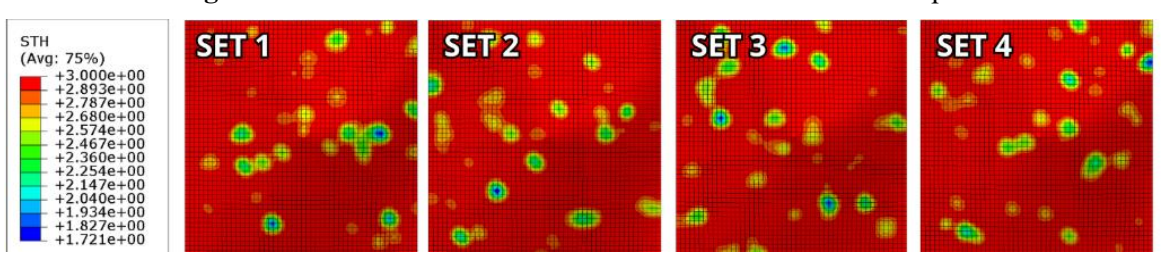


Figure 8. Thickness contour of a 36-month-immersed corroded plate

The outcomes of the randomization process in each set demonstrate variability in contour distribution, indicating that the initial corrosion positions in the simulation are entirely random. The color gradation from blue, green, and yellow to red indicates varying depths in localized regions, suggesting that the modeled corrosion attacks the metal surface in a highly localized manner. As shown in Figures 6-8, there are discernible variations in the number of pits and the distribution of corroded regions across the plate surface. This observation supports the progressive nature of the corrosion process, in which corrosion pits grow, coalesce, and ultimately result in substantial thickness reduction during immersion.

3.2 Displacement response of corroded plate

The mechanical response of plates subjected to corrosion was evaluated using two approaches. First, the immersion period was varied to observe the progressive nature of degradation over time. Second, the pit locations were randomized to assess potential positions that produce the most critical mechanical responses. This study focuses on a plate model subjected to a centralized load at immersion periods of 6, 12, and 36 months, each with four variations of pit position randomization. The analysis includes the effects of corrosion on maximum displacement, strain, and von Mises stress values. As shown in Figure 9, the mechanical response contours are presented for both the undegraded plate and the corroded plates after 6, 12, and 36 months of immersion. The figure illustrates the displacement (a-d), strain (e-h), and von Mises stress (i-l) contours for each immersion period and randomization set.

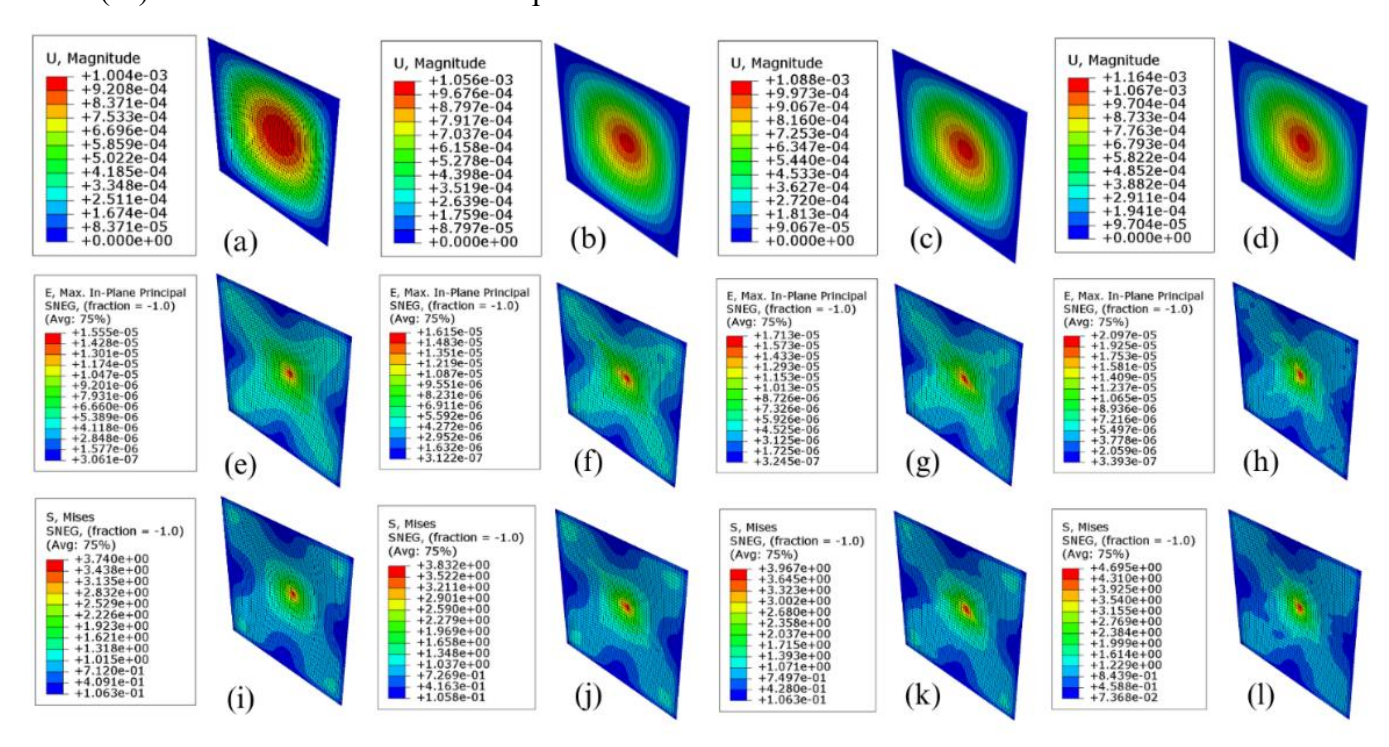


Figure 9. Comparison of mechanical response contours of corroded plates: (a-d) Displacement contours for 0, 6, 12, and 36 months; (e-h) Strain contours for 0, 6, 12, and 36 months; (i-l) Von Mises stress contours for 0, 6, 12, and 36 months

As shown in Figure 10, the randomization of pit locations produces a wide range of mechanical responses. Figure 10a presents the maximum displacement, Figure 10b shows the strain, and Figure 10c illustrates the von Mises stress. The variation in these results is primarily due to the presence of pits in specific high-response regions under the concentrated load, which leads to differences in the distribution of structural responses. For example, at 36 months, Set 4 exhibits the highest values 1.227×10^{-3} mm (displacement), 2.290×10^{-5} (strain), and 4.963 MPa (von Mises stress). This is attributed to the strategic placement of pits in Set 4, located at the plate center and along its diagonal, which are critical stress zones as shown in Figure 9. The thickness contour supports this observation, as shown in Figure 6, which shows that pits in Set 4 predominantly occupy these critical regions.

In contrast, Set 2 at 36 months records the lowest responses 1.152×10^{-3} mm (displacement), 1.806×10^{-5} (strain), and 4.152 MPa (von Mises stress), highlighting the importance of pit location in determining the severity of structural degradation. Overall, corrosion resulted in a progressive weakening effect over time. The mean maximum displacement increased from 1.051×10^{-3} mm at 6 months to 1.078×10^{-3} mm at 12 months and 1.175×10^{-3} mm at 36 months. Similarly, the mean strain values increased from 1.594×10^{-5} to 1.656×10^{-5} and 2.035×10^{-5} , while the mean von Mises stress rose from 3.811 MPa to 3.930 MPa and 4.493 MPa over the same periods.

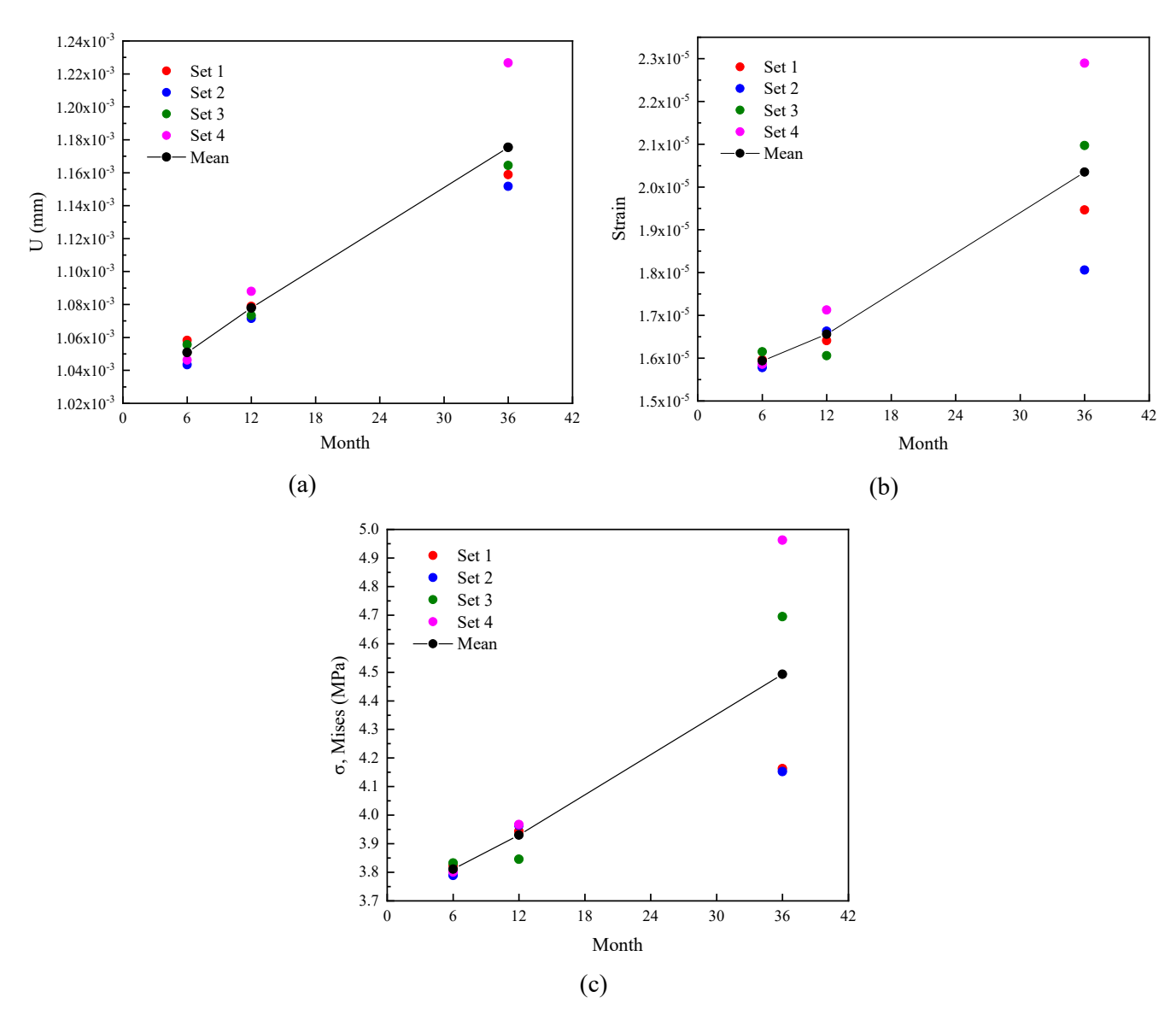


Figure 10. Mechanical response of corroded plate: (a) Displacement, (b) Strain, and (c) Von Mises stress

The trend shown in Figure 11 confirms the progressive effect of corrosion, as all response parameters increased consistently with immersion time. This demonstrates that corrosion-induced degradation substantially reduces the structural capacity of the plate when subjected to concentrated loading, with severity increasing as pits expand and coalesce in critical stress regions. A comparative analysis shows that all three mechanical response parameters of the corroded plates increased relative to the corrosion-free condition. After 6, 12, and 36 months of immersion, the maximum displacement rose by 4.84%, 7.54%, and 17.27%, respectively. Over the same periods, strain increased by 2.45%, 6.44%, and 30.8%, while von Mises stress increased by 1.9%, 5.07%, and 20.12%, respectively. These results confirm that prolonged corrosion exposure significantly degrades the structural performance of the plate under concentrated loading, with the severity of the degradation intensifying over time.

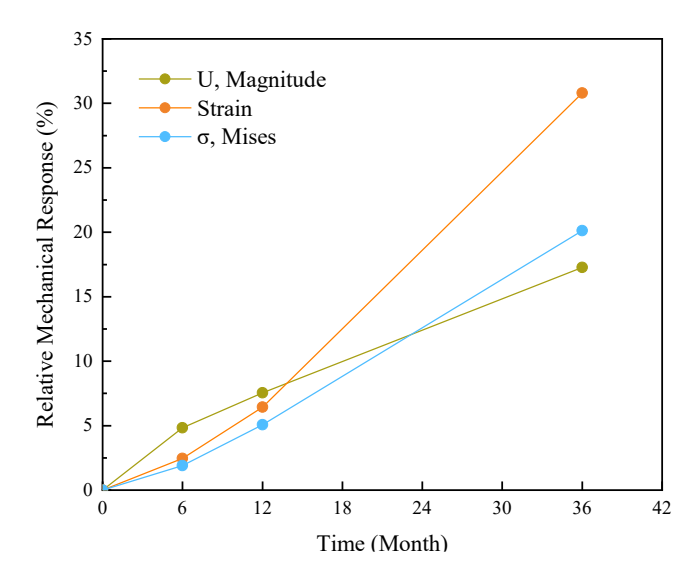


Figure 11. Trendline of the relative average mechanical response of the corroded plate

4 Conclusions

The present study evaluates the alterations in the mechanical response of plates subjected to crevice corrosion. Utilizing data from the immersion of plates exposed to barnacle attachment and loaded with a centralized force, the study aims to achieve a comprehensive understanding of the underlying mechanisms using the finite element method. A total of 12 simulations were executed, considering the variation in pit geometry based on immersion duration, as well as the random position of the pits within each randomization set. The primary outcomes demonstrate that crevice corrosion modeling can be expeditiously implemented in ABAQUS through the analytical mapped field feature, thereby obviating the need for manually redesigning the pit geometry individually. The variation in pit geometry, influenced by the duration of immersion, has a significant impact on the relative mechanical response trends, particularly concerning the depth, area, and number of pits that extend onto the metal surface. The data distribution of the four randomization sets exhibited significant disparities, with 36 months of immersion resulting in a more pronounced dispersion of data between sets compared to the previous period. This phenomenon can be attributed to the augmented number of pits, which modifies the plate's response to external loads. Consequently, the probability of observing a high response is increased, particularly in areas with critical values within the simulated contours. This finding can inform the development of corrosion models and evaluation methods for the mechanical response caused by corrosion.

Based on these findings, it is recommended that future structural assessments of corroded marine components incorporate realistic corrosion geometries obtained from in-situ measurements, as demonstrated in this study. Additionally, long-term monitoring under varying environmental and loading conditions is recommended to further validate and extend the numerical modeling approach presented herein.

References

- 1. G. H. Koch, M.P. H. Brongers, and N. G. Thompson, *Corrosion Cost and Preventive Strategies in the United States*, Virginia: U.S. Federal Highway Administration, 2001.
- 2. B. Hou, X. Li, X. Ma, C. Du, D. Zhang, M. Zheng, W. Xu, D. Lu, and F. Ma, "The Cost of Corrosion in China", *npj Mater. Degrad.*, vol. 1, article no. 2, 2017.
- 3. S. Kainuma, Y. S. Jeong, and J. H. Ahn, "Investigation on the stress concentration effect at the corroded surface achieved by atmospheric exposure test," *Mater. Sci. Eng.*, vol. 602, pp. 89-97, 2014.
- 4. A. J. Betts and L. H. Boulton, "Crevice corrosion: Review of mechanisms, modelling, and mitigation," *Br. Corros. J.*, vol. 28, no. 4, pp. 279-295, 1993.
- 5. A. S. H. Makhlouf and M. A. Botello, *Chapter 1-Failure of the Metallic Structures due to Microbiologically induced corrosion and the techniques for protection*, Oxford: Butterworth-Heinemann, 2018.
- 6. Z. Ahmad, *Principles of Corrosion Engineering and Corrosion Control*, Oxford: Butterworth-Heinemann, 2006.

- 7. L. D. Chambers, K. R. Stokes, F. C. Walsh, and R. J. K. Wood, "Modern approaches to marine antifouling coatings," *Surf. Coatings Technol.*, vol. 201, no. 6, pp. 3642-3652, 2006.
- 8. K. K. Satpathy, A. K. Mohanty, G. Sahu, S. Biswas, and M. Selvanayagam, "Biofouling and its Control in Seawater Cooled Power Plant Cooling Water System A Review," *Nucl. Power*, vol. 11, pp. 192-234, 2010.
- 9. B. J. Little and J. S. Lee, *Microbiologically Influenced Corrosion*, New Jersey: John Wiley & Sons., 2009.
- 10. T. Nakai, H. Matsushita, N. Yamamoto, and H. Arai, "Effect of pitting corrosion on local strength of hold frames of bulk carriers (1st report)," *Mar. Struct.*, vol. 17, no. 5, pp. 403-432, 2004.
- 11. T. Nakai, H. Matsushita, and N. Yamamoto, "Effect of pitting corrosion on strength of web plates subjected to patch loading," *Thin-Walled Struct.*, vol. 44, no. 1, pp. 10-19, 2006.
- 12. A. A. Pratama, A. R. Prabowo, T. Muttaqie, N. Muhayat, R. Ridwan, B. Cao, and F. B. Laksono, "Hollow tube structures subjected to compressive loading: implementation of the pitting corrosion effect in nonlinear FE analysis," *J. Braz. Soc. Mech. Sci. Eng.*, vol. 45, article no. 143, 2023.
- 13. L. D. Sarno, A. Majidian, and G. Karagiannakis, "The effect of atmospheric corrosion on steel structures: A state-of-the-art and case-study," *Build.*, vol. 11, no. 12, article no. 571, 2021.
- 14. J. Zhang, X. H. Shi, and C. G. Soares, "Experimental analysis of residual ultimate strength of stiffened panels with pitting corrosion under compression," *Eng. Struct.*, vol. 152, pp. 70-86, 2017.
- 15. Z. Zhang, Z. Li, F. Wu, J. Xia, K. Huang, B. Zhang, and J. Wu, "A comparison study of crevice corrosion on typical stainless steels under biofouling and artificial configurations," *npj Mater. Degrad.*, vol. 6, no. 1, article no. 85, 2022.
- 16. Y. Sharifi, S. Tohidi, and J. K. Paik, "Ultimate compressive strength of deteriorated steel web plate with pitting and uniform corrosion wastage," *Scientia Iranica*, vol. 23, no. 2, pp. 486-499, 2016.
- 17. Z. Zhao, B. Liang, H. Liu, and X. Wu, "Influence of pitting corrosion on the bending capacity of thin-walled circular tubes" *J. Braz. Soc. Mech. Sci. Eng.*, vol. 40, article no. 548, 2018.
- 18. M. Kutz, Mechanical Engineers' Handbook: Materials and Mechanical Design: Third Edition, New Jersey: John Wiley & Sons, 2006.
- 19. H. S. Alsos and J. Amdahl, "On the resistance to penetration of stiffened plates, Part I Experiments," *Int. J. Impact Eng.*, vol. 36, no. 6, pp. 799-807, 2009.